ISSN 1070-4280, Russian Journal of Organic Chemistry, 2023, Vol. 59, No. 10, pp. 1714–1724. © The Author(s), 2023. This article is an open access publication.
Russian Text © The Author(s), 2023, published in Zhurnal Organicheskoi Khimii, 2023, Vol. 59, No. 10, pp. 1363–1374.

Dedicated to Full Member of the Russian Academy of Sciences B.A. Trofimov on his 85th anniversary

Theoretical Study of the Electronic Structure and Ionization Spectrum of γ-Pyrone

A. B. Trofimov[a,b,*], E. K. Iakimova[b], E. V. Gromov[b,c], and A. D. Skitnevskaya[b]

[a] *Favorskii Irkutsk Institute of Chemistry, Siberian Branch, Russian Academy of Sciences, Irkutsk, 664033 Russia*

[b] *Irkutsk State University, Irkutsk, 664003 Russia*

[c] *Max-Planck Institute for Medical Research, Heidelberg, 69120 Germany*

**e-mail: abtrof@mail.ru*

Received August 15, 2023; revised August 25, 2023; accepted August 26, 2023

Abstract—The electronic structure and ionization spectrum of γ-pyrone (4*H*-pyran-4-one) were calculated using the third-order algebraic diagrammatic construction method for the single-particle Green function [IP-ADC(3)] and some other high-level quantum chemical methods. The results of calculations were used to interpret its recently recorded photoelectron spectra. New assignments have been proposed for the nature of a series of photoelectron maxima of γ-pyrone located above 12 eV, where, according to calculations, the one-electron ionization pattern is disturbed due to electron correlation effects. The obtained results significantly change the interpretation of the spectrum available in the literature.

Keywords: γ-pyrone, 4*H*-pyran-4-one, electronic structure, photoelectron spectra, ionization, quantum chemical calculations, IP-ADC(3), IP-EOM-CCSD, SAC-CI

DOI: 10.1134/S1070428023100068

INTRODUCTION

γ-Pyrone (4*H*-pyran-4-one) is one of the fundamental conjugated heterocyclic molecules that play an important role in the construction of biological systems and compounds with pharmacophore properties (Fig. 1). The synthesis of pyrones and study of their properties are the subjects of ongoing research [1–5]. A recent example is an efficient one-pot synthesis of substituted pyrones from acetylenes discovered under the leadership of B.A. Trofimov [6, 7].

The electronic structure of pyrones has attracted significant interest. Herein, π-electrons of the double bonds of the pyran ring are conjugated with lone electron pairs of the ring oxygen atom and carbonyl oxygen, which may be represented by the corresponding neutral and zwitterionic resonance structures (Fig. 1). Therefore, fairly strong electron correlation effects can be expected, which should be reflected primarily in the ionization spectra. This is confirmed by the photoelectron spectra of γ-pyrone [8] recently obtained at Elettra Sincrotrone Trieste, which showed broad bands above 12 eV; these bands were interpreted as complex combinations of the main and satellite lines.

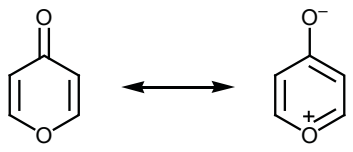

Fig. 1. Resonance structures of γ-pyrone.

It is well known that satellite transitions are an integral part of any ionization spectrum and that their appearance is related to disturbance of the single-electron ionization picture [9]. The latter applies to the main lines that represent processes of electron ionization from one of the occupied orbitals with the formation of one-hole configurations (*h*). Satellites correspond to more complex processes, where removal of one electron is accompanied by excitation of another

with the formation of configuration like two holes–one particle ($2h$–$1p$). The intensity of satellite transitions is borrowed from the main lines, which can be interpreted as mixing of h and $2h$–$1p$ configurations. In most cases, this configuration interaction begins to be observed in the region of 12–15 eV. As the ionization energy increases, it becomes more and more significant, leading to an increase in the number of satellites and band broadening [9].

In view of the stated above, the interpretation of the photoelectron spectrum of γ-pyrone proposed in [8] on the basis of SAC-CI (symmetry-adapted cluster–configuration interaction) calculations [10–12] seems rather strange, as it predicts the occurrence of only electronic transitions corresponding to ionization of 12 orbitals of γ-pyrone with complete absence of satellite lines throughout the entire outer-valence ionization region (≤18–19 eV).

In order to establish the real physical picture, in this work we studied the outer valence ionization of γ-pyrone using the well-proven third-order algebraic diagrammatic construction method for the single-particle Green function [IP-ADC(3)] [13–17]. The results were compared with the experimental data given in [8], as well as with the results of calculations by the IP-EOM-CCSD (equation of motion coupled-cluster singles and doubles for the calculation of ionization potentials) [18–20] method which is equivalent to SAC-CI. For some low-lying transitions, the relation between the ionization energy and the basis set and theoretical level of electronic structure description was studied.

RESULTS AND DISCUSSION

Table 1 shows the results of calculation of the six lower vertical ionization energies of γ-pyrones by different methods using different basis sets. Each of the corresponding cationic states can be unambiguously ascribed to one of the molecular orbitals (MO) of γ-pyrone whose structure is illustrated in Fig. 2. The orbitals were calculated according to the Hartree–Fock (HF) method according to which the electronic configuration of γ-pyrone is as follows:

$$[\text{core part}]\ 10a_1^2\ 5b_2^2\ 11a_1^2\ 1b_1^2\ 6b_2^2\ 12a_1^2\ 7b_2^2\ 13a_1^2\ 2b_1^2\ 8b_2^2\ 1a_2^2\ 3b_1^2,$$

where the MOs are numbered in terms of the C_{2v} point symmetry group to which γ-pyrone belongs, and the core part includes all core and inner valence orbitals.

The vertical ionization energies significantly change when going from the HF method (Koopmans' theorem) to correlation methods (Table 1), and in some cases, disagreement even in the sequences of MOs (cationic state) is observed. Strong electron correlation effects for γ-pyrone are also reflected in the fact that such disagreement is retained for high-level calculations. In particular, comparison of the states in the pairs 1^2B_1 $(3b_1^{-1})$/1^2B_2 $(8b_2^{-1})$ and 2^2B_1 $(2b_1^{-1})$/1^2A_1 $(13a_1^{-1})$ shows that the sequence predicted by IP-ADC(3) is opposite to that determined by IP-EOM-CCSD.

In order to reliably determine the sequence of low-energy vertical electronic transitions in the ionization spectrum of γ-pyrone, the calculations were carried out using the CC3 method which is one of the most accurate today. The results (Table 1) showed the following sequence in the above discussed pairs of cationic states: 1^2B_2 $(8b_2^{-1})$/1^2B_1 $(3b_1^{-1})$ and 2^2B_1 $(2b_1^{-1})$/1^2A_1 $(13a_1^{-1})$.

However, the energies of transitions calculated at the CC3/cc-pVTZ level are still quite far from the experimental values, which is due to the basis set error. The latter stems from the fairly large corrections for the incompleteness of cc-pVTZ basis set (Δ_{TZ}), determined by extrapolation to the complete basis set (CBS) limit in the OVGF method (Table 1). The best theoretical estimates (BTE) for the CC3 method with complete basis set can be obtained by combining Δ_{TZ} with the CC3/cc-pVTZ approximation data (Table 1). Since in the experimental spectrum the first two transitions give one peak, the average of their calculated energies (9.48 eV) should be compared with the experimental value. The third transition with a BTE energy of 10.92 eV gives an individual peak. Likewise, the average of the BTE energies (13.36 eV) should again be considered for the fourth to sixth transitions that contribute to the third peak. These estimates are in good agreement with the positions of photoelectron maxima given in [8]: 9.5, 10.9, and 13.1 eV, respectively, especially in the case of two low-energy peaks.

The photoelectron spectrum in the entire outer valence range was simulated using aug-cc-pVTZ basis set including diffuse functions necessary to describe the satellite states which, as mentioned above, were the focus of our study. The calculation results and spectral envelopes simulated by the IP-ADC(3) and IP-EOM-CCSD methods are compared with the experimental data in Figs. 3 and 4, respectively. More detailed results are given in Table 2.

The IP-ADC(3) spectral envelope reproduces the experimental spectrum with a good quality. The theo-

Table 1. Energies (eV) of vertical transitions involving six lowest cationic states of γ-pyrone, calculated by different methods with different basis sets, in comparison with the experimental data and results of previous theoretical calculations

Method	Basis set	$1\,^2B_2$	$1\,^2B_1$	$1\,^2A_2$	$2\,^2B_1$	$1\,^2A_1$	$2\,^2B_2$
		$(8b_2^{-1})$	$(3b_1^{-1})$	$(1a_2^{-1})$	$(2b_1^{-1})$	$(13a_1^{-1})$	$(7b_2^{-1})$
HF (Koopmans)	cc-pVTZ	11.37	9.93	10.99	14.61	15.13	15.46
IP-ADC(3)		9.79	9.42	10.91	12.89	13.63	14.01
IP-EOM-CCSD		9.43	9.54	11.03	13.43	13.34	13.96
CC3		9.13	9.43	10.78	12.87	13.10	13.58
HF (Koopmans)	aug-cc-pVTZ	11.46	10.01	11.05	14.69	15.18	15.51
IP-ADC(3)		9.91	9.54	10.99	13.00	13.72	14.09
IP-EOM-CCSD		9.55	9.65	11.11	13.53	13.43	14.04
IP-EOM-CCSD	6-311G**	9.19	9.32	10.92	13.24	13.16	13.83
SAC-CI[a]		9.19	9.28	10.78	13.23	13.37	13.85
OVGF	cc-pVDZ	9.46	9.17	10.64	13.28	13.23	13.75
	cc-pVTZ	9.77	9.42	10.83	13.49	13.45	13.96
	cc-pVQZ	9.90	9.53	10.91	13.59	13.56	14.05
	cc-pV5Z	9.95	9.57	10.94	13.62	13.61	14.08
	cc-pV$_\infty$Z[b]	9.99	9.60	10.97	13.66	13.66	14.13
	aug-cc-pVDZ	9.88	9.52	10.82	13.60	13.61	14.02
	aug-cc-pVTZ	9.94	9.56	10.91	13.61	13.61	14.06
	aug-cc-pVQZ	9.97	9.59	10.94	13.63	13.63	14.09
	aug-cc-pVZ[b]	10.00	9.61	10.96	–	–	14.11
	CBS[c]	10.00	9.60	10.97	13.66	13.66	14.12
	Δ_{TZ}[d]	0.23	0.18	0.14	0.17	0.20	0.16
BTE[e]		9.36	9.61	10.92	13.04	13.30	13.74
		9.48				13.36	
Experimental data[f]		9.5		10.9		13.1	

[a] Data of [8].

[b] Extrapolation to the complete basis set limit for the sequence of basis sets.

[c] Expected value for the complete basis set, calculated as the average of the sequences cc-pVxZ and aug-cc-pVxZ.

[d] Correction for incompleteness of the cc-pVTZ basis set.

[e] Best theoretical estimate (sum of the transition energy calculated at the CC3/cc-pVTZ level and the correction Δ_{TZ}); for the transitions contributing to the same peak, the average energy is also given for convenience in comparison with the experimental data.

[f] Experimental positions of maxima in the photoelectron spectrum were taken from [8].

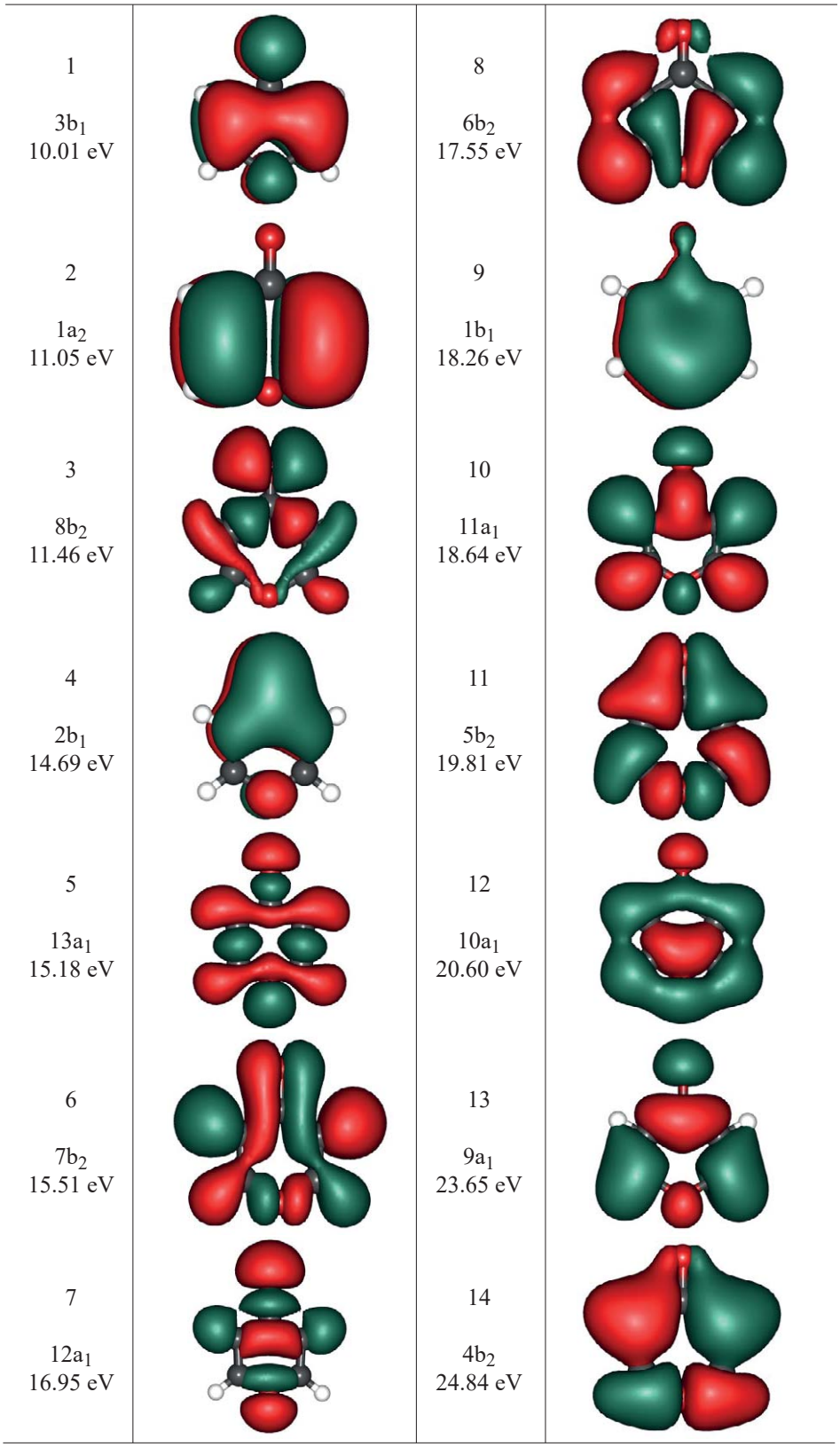

Fig. 2. Higher occupied molecular orbitals of γ-pyrone (from HOMO to HOMO-13) and their symmetries and energies according to HF/aug-cc-pVTZ calculations.

retical envelope reproduces not only the relative positions of spectral maxima but also their shape. It is clearly seen (Fig. 3) that broadening of the maxima is caused by the appearance of photoelectron satellites at about 14 eV, whose intensity increases with increase in energy. Taking into account that the mechanism of appearance of satellites implies borrowing intensities from the main lines, some main transitions in the spectrum are appreciably weakened, which leads to the appearance of specific forms of maxima. Overall, all this is typical of outer valence ionization spectra which demonstrate breakdown of the orbital ionization picture in the mid- and high-energy regions of the spectrum [9].

The observed agreement between the theoretical and experimental spectra allows for the interpretation and assignment of the experimental data at a good quality level.

As we already discussed above, maximum A in the experimental spectrum with an energy of ~9.5 eV arises from two closely located transitions $8b_2^{-1}$ (1^2B_2) and $3b_1^{-1}$ (1^2B_1), whose sequence is indicated here in accordance with the most accurate data of the CC3 method. The IP-ADC(3) calculations give the reverse order of these transitions since the 1^2B_2 ($8b_2^{-1}$) state has an energy exceeding by 0.6 eV the energy predicted by CC3 calculations (Table 1). In this case, the large error of the IP-ADC(3) method relates to the fact that the MO $8b_2$ is associated with the *n*σ type lone electron pair (LEP) of the carbonyl oxygen atom (Fig. 2). Ionization of such orbitals is accompanied by strong relaxation effects [17] [the state 1^2B_2 ($8b_2^{-1}$) changes from the third at the HF level to first at the CC3 level], which does not allow good results to be obtained by less accurate methods. As can be seen, this result actually means that the *n*σ-LEP on the carbonyl oxygen (8b2) can be considered as the highest occupied molecular orbital (HOMO), followed by the π-bond orbitals 3b1 and 1a2, as far as ionization processes, and reactions where γ-pyrone acts as a σ-donor, are concerned.

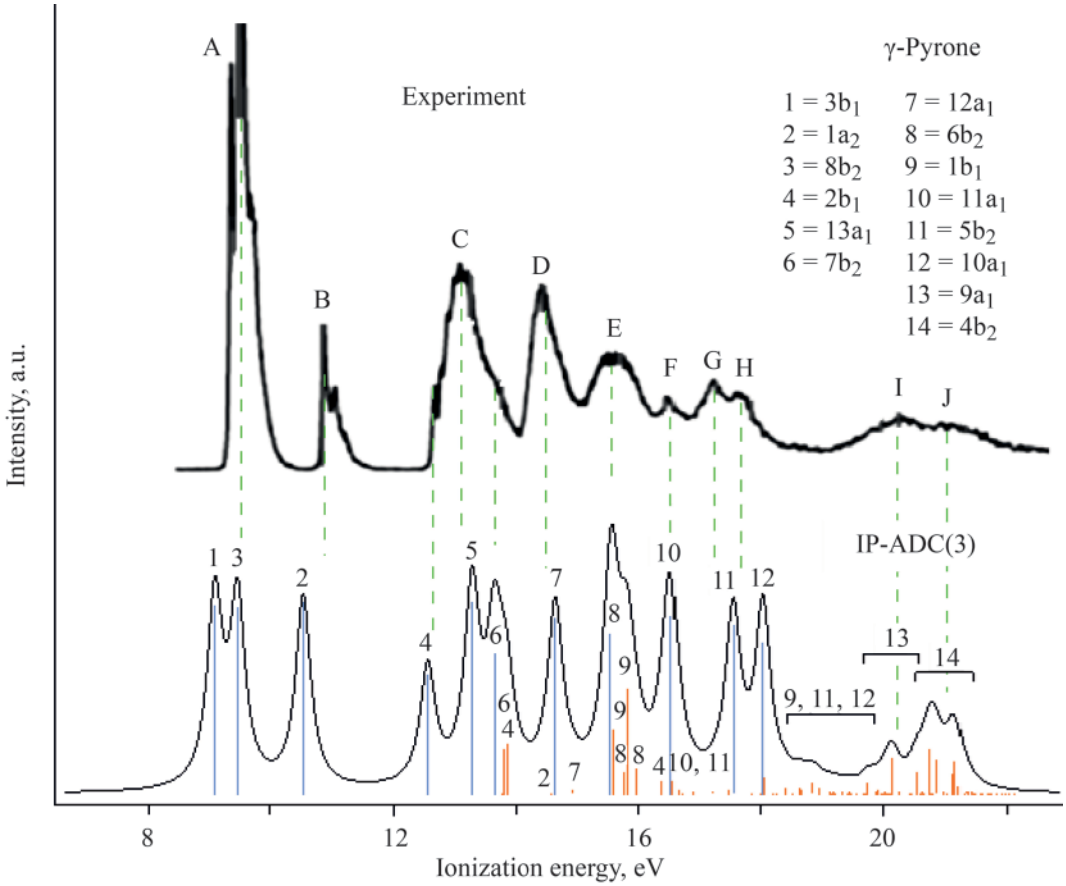

Fig. 3. Theoretical [IP-ADC(3)/aug-cc-pVTZ] and experimental ionization spectra of γ-pyrone. The theoretical spectrum is shifted by –0.30 eV relative to the experimental spectrum; vertical transitions that can be considered as main lines ($P \geq 0.5$) are shown in blue, and those corresponding to satellite lines ($P < 0.5$) are shown in red.

Table 2. Energies (E, eV) and intensities (P) of 30 low-lying vertical transitions of γ-pyrone, calculated by the IP-ADC(3)/aug-cc-pVTZ methods, in comparison with those obtained by the IP-EOM-CCSD/aug-cc-pVTZ method and experimental data

State	Configuration[a]		ADC(3)		CCSD		Experimental value[b]
			E	P	E	P	E
$1\,^2B_1$	$3b_1^{-1}$		9.54	0.87	9.65	0.93	9.5 (A)
$1\,^2B_2$	$8b_2^{-1}$		9.91	0.85	9.55	0.91	
$1\,^2A_2$	$1a_2^{-1}$		10.99	0.88	11.11	0.94	10.9 (B)
$2\,^2B_1$	$2b_1^{-1}$		13.00	0.54	13.53	0.89	
$1\,^2A_1$	$13a_1^{-1}$		13.72	0.88	13.43	0.92	
$2\,^2B_2$	$7b_2^{-1}$		14.09	0.64	14.04	0.92	
$2\,^2A_1$	$13a_1^{-1}$	$8b_2^{-1}\ 1a_2^{-1}\ 5b_1$	14.23	< 0.01			13.1 (C)
$3\,^2B_2$	$7b_2^{-1}$	$8b_2^{-1}\ 3b_1^{-1}\ 5b_1$	14.25	0.20			
$2\,^2A_2$	$1a_2^{-1}$	$3b_1^{-1}\ 3b_1^{-1}\ 2a_2$	14.29	0.01			
$3\,^2B_1$	$2b_1^{-1}$	$3b_1^{-1}\ 3b_1^{-1}\ 5b_1$	14.31	0.22			
$3\,^2A_2$	$1a_2^{-1}$	$1a_2^{-1}\ 3b_1^{-1}\ 5b_1$	15.02	0.01			
$3\,^2A_1$	$12a_1^{-1}$		15.10	0.81	14.72	0.90	14.5 (D)
$4\,^2A_1$	$12a_1^{-1}$	$1a_2^{-1}\ 8b_2^{-1}\ 5b_1$	15.37	0.02			
$4\,^2B_2$	$6b_2^{-1}$		16.00	0.74	16.05	0.92	
$4\,^2B_1$	$1b_1^{-1}$	$1a_2^{-1}\ 1a_2^{-1}\ 5b_1$	16.05	0.29			
$5\,^2B_2$	$6b_2^{-1}$	$8b_2^{-1}\ 1a_2^{-1}\ 2a_2$	16.23	0.10			15.6 (E)
$5\,^2B_1$	$1b_1^{-1}$	$3b_1^{-1}\ 1a_2^{-1}\ 2a_2$	16.28	0.48	16.07	0.89	
$6\,^2B_2$	$6b_2^{-1}$	$8b_2^{-1}\ 1a_2^{-1}\ 2a_2$	16.43	0.12			
$6\,^2B_1$	$2b_1^{-1}$	$8b_2^{-1}\ 8b_2^{-1}\ 5b_1$	16.85	0.06			
$5\,^2A_1$	$11a_1^{-1}$		16.97	0.82	16.99	0.91	
$7\,^2B_1$	$2b_1^{-1}$	$8b_2^{-1}\ 8b_2^{-1}\ 5b_1$	17.01	0.06			
$6\,^2A_1$	$11a_1^{-1}$	$8b_2^{-1}\ 3b_1^{-1}\ 2a_2$	17.09	0.02			16.5 (F)
$4\,^2A_2$	$1a_2^{-1}$	$1a_2^{-1}\ 2b_1^{-1}\ 5b_1$	17.17	<0.01			
$5\,^2A_2$	$1a_2^{-1}$	$1a_2^{-1}\ 3b_1^{-1}\ 5b_1$	17.33	0.01			
$7\,^2B_2$	$5b_2^{-1}$	$7b_2^{-1}\ 3b_1^{-1}\ 5b_1$	17.64	0.01			
$7\,^2A_1$	$11a_1^{-1}$	$13a_1^{-1}\ 3b_1^{-1}\ 5b_1$	17.92	0.01			17.2 (G)
$8\,^2B_2$	$5b_2^{-1}$		17.99	0.78	17.72	0.90	
$6\,^2A_2$	$1a_2^{-1}$	$13a_1^{-1}\ 8b_2^{-1}\ 5b_1$	18.29	<0.01			
$9\,^2B_2$	$5b_2^{-1}$	$13a_1^{-1}\ 1a_2^{-1}\ 5b_1$	18.44	<0.01			17.7 (H)
$8\,^2A_1$	$10a_1^{-1}$		18.47	0.70	18.34	0.90	

[a] For the states with predominant $2h$–$1p$ configuration, the most important h configuration responsible for the intensity of the corresponding transition is also given in addition to $2h$–$1p$.

[b] Data of [8]; see Figs. 3 and 4.

According to the available theoretical data, the well-separated photoelectron maximum with an energy of ~10.9 eV can be unambiguously assigned to the $1a_2^{-1}$ (1^2A_2) transition corresponding to ionization of the second π orbital.

The assignment of the C band with its maximum at about 13.1 eV is more difficult, since this band extends to a significant range of 12.5–14 eV and has two clearly defined shoulders at ~12.7 and ~13.7 eV. As follows from the IP-ADC(3) calculations, this spectral region is formed by seven transitions, three of which are the main ones and the other four are satellite (Table 2). The main lines correspond to ionization of the $2b_1$, $13a_1$, and $7b_2$ orbitals. The satellites originate from transitions leading to the formation of vacancies at *n*σ-MO and highest π-MO and population of π*-MO, whose intensities are borrowed from the main transitions $2b_1^{-1}$ and $7b_2^{-1}$. The results of our simulation (Fig. 3) showed that it is the latter two transitions with appreciably reduced intensities that are responsible for the shoulders with energies of ~12.7 and ~13.7 eV. The high-energy shoulder has also contributions from by satellite transitions. This is consistent with the CC3 calculation data, which predicted for the C band the same sequence of the main states as the IP-ADC(3) method, as well as qualitatively similar distribution of the relative intensities $P(2b_1^{-1}):P(13a_1^{-1}):P(7b_2^{-1})$ = 0.81:1:0.95 [0.61:1:0.73 in the case of IP-ADC(3)]. Although the satellite transitions contributing to the C band were not calculated by the CC3 method (because of high computational costs), the given data clearly indicate that they are located somewhere nearby, since they acquired the missing part of the intensity of $2b_1^{-1}$ and $7b_2^{-1}$. The given interpretation of the C band is quite different from that proposed in [8], where it was attributed to only three main transitions with equal intensities on the basis of SAC-CI calculations.

We assigned the D band with its maximum at about 14.5 eV to the $12a_1^{-1}$ transition accompanied by two low-intensity satellites (Table 2). A similar assignment, but without satellites, was proposed in [8]. The assumption that the D band has contributions from the state 2^2B_2 ($7b_2^{-1}$), based on multiconfiguration HF (CASSCF) calculations [8], seems hardly realistic, since in this case the intensity of the D band would be doubled, which is not observed experimentally.

The E band with its maximum at about 15.6 eV in the experimental spectrum is rather diffuse, and it appears in the region of 15.1–16.2 eV. Its shape is well explained by our IP-ADC(3) calculations, according to which the E band has contributions from a large number of satellite transitions that borrow intensity from the deeply lying π-MO $1b_1$. Due to the strong intensity transfer to the satellites, the main $1b_1^{-1}$ line is completely absent in the ionization spectrum of γ-pyrone (Fig. 3, Table 2); this is often observed in the spectra of conjugated heterocycles [21]. According to our data, the other part of the intensity of that band is provided by the $6b_2^{-1}$ (4^2B_2) transition. Once again, SAC-CI calculations [8] do not predict contributions of satellites, and the E band was treated as originating exclusively from the $6b_2^{-1}$ and $1b_1^{-1}$ transitions.

A small peak F in the region of ~16.5 eV was interpreted by us as the result of electron ionization from the $11a_1$ orbital. Our calculations predict the presence of some satellites in the vicinity of the corresponding main line; however, the intensity of these satellites is insignificant.

A similar situation is predicted for the G and H maxima observed in the spectrum at ~17.2 and ~17.7 eV, respectively. These maxima arise from ionization of the $5b_2$ and $10a_1$ orbitals, respectively. As in the case of the F peak, the contribution of satellites to the G and H bands is insignificant, though their existence is predicted by our calculations.

According to the IP-ADC(3) data, the region above 18 eV is characterized by total breakdown of the orbital ionization picture, which is consistent with the generally accepted views on the structure of photoelectron spectra [9]. Here, the spectral envelope is the result of a large number of low-intensity 2*h*–1*p* satellite transitions arising from interactions with *h*-type transitions which correspond to ionization of MOs with appropriate energies. The main lines corresponding to orbital ionization no longer appear in this part of the spectrum, and the resulting states have a complex multielectron nature.

The results of SAC-CI calculations [8] were verified using the IP-EOM-CCSD method which is equivalent to SAC-CI. Table 1 compares the obtained results with the SAC-CI/6-311G** data [8]. As expected, the results are in good agreement with each other, and the existing small discrepancies are most likely to be due to differences in the geometric parameters and basis set limitations in the SAC-CI calculations [8]. The wide-range spectrum calculated by the IP-EOM-CCSD method reproduces the SAC-CI data [8] together with the problems associated with the latter (Fig. 4, Table 2). As noted above, the main problem is

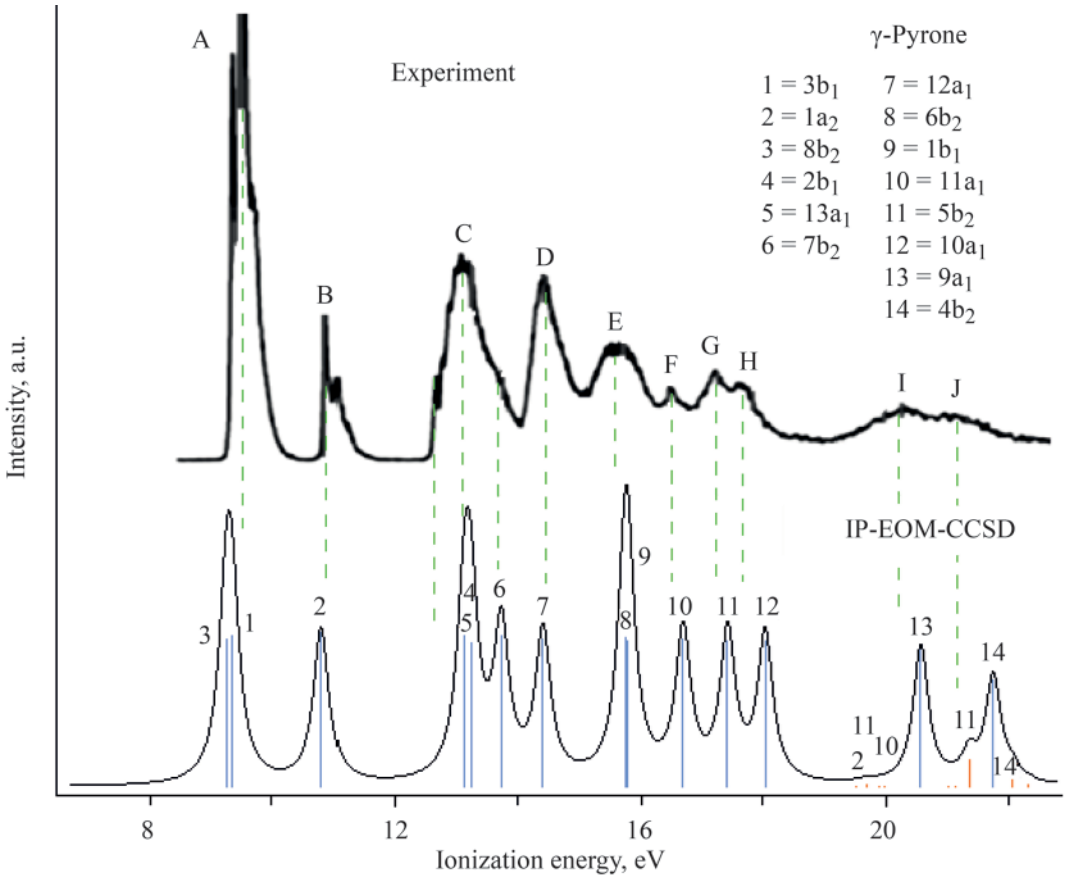

Fig. 4. Theoretical [IP-EOM-CCSD/aug-cc-pVTZ] and experimental ionization spectra of γ-pyrone. The theoretical spectrum is shifted by –0.46 eV relative to the experimental spectrum; vertical transitions that can be considered as main lines ($P \geq 0.5$) are shown in blue, and those corresponding to satellite lines ($P < 0.5$) are shown in red.

that the spectrum below ~19 eV is represented exclusively by main lines without satellite transitions and variation of the main line intensities. As far as we know, this feature of the IP-EOM-CCSD and SAC-CI methods has not been discussed previously in the literature, and it requires more thorough theoretical analysis.

EXPERIMENTAL

The energies (E) and relative intensities (P) of vertical transitions in the ionization spectra were calculated by the IP-ADC(3) [13–15] and IP-EOM-CCSD [18–20] methods using 6-311G** [22, 23], cc-pVTZ, and aug-cc-pVTZ basis sets [24, 25]. The calculations were carried out using Q-Chem software package [26]. The geometric parameters of γ-pyrone used in the calculations were optimized in the framework of the second order Møller–Plesset perturbation theory (MP2) with cc-pVTZ basis set using Gaussian [27]. The spectral envelopes were constructed by convolution of the calculated energies and intensities of vertical transitions with Lorentzian functions with a line half-width of 0.3 eV. The molecular orbitals were visualized with the aid of Molden [28].

The energies of four low-lying vertical transitions of γ-pyrone were also calculated by the linear response coupled cluster singles and doubles method including perturbation of triply excited configurations with the linear response function perturbative correction for triply excited configurations (CC3) [29–31], which is more accurate than IP-ADC(3) and IP-EOM-CCSD. The calculations were performed by CFOUR software [32] using cc-pVTZ basis set.

The dependence of the energy of low-lying vertical transitions on the basis set was clarified using the outer-valence Green's function (OVGF) method [33–35], which is somewhat less rigorous in theoretical terms but more economical in terms of computational resources than IP-ADC(3). Two series of basis sets, cc-pVxZ (x = D, T, Q, 5) and aug-cc-pVxZ (x = D,

T, Q) [24, 25] were used, and the results obtained in each case were then extrapolated to the complete basis set (CBS) limit [36, 37]. The calculations were carried out using Gaussian.

CONCLUSIONS

The results of high-level quantum chemical calculations [IP-ADC(3), IP-EOM-CCSD, CC3, OVGF] showed that the electronic structure of γ-pyrone is quite complex due to electron correlation effects. These effects are reflected in the complex structure of the ionization spectrum and disagreement between the high-level methods with respect to the sequence of cationic states and origin of spectral lines.

Another evidence of the importance of many-electron effects is the significant role of satellites in the ionization spectrum, which is clearly demonstrated by IP-ADC(3) calculations. Intensity redistribution from the main lines to satellites is observed starting from ~12 eV, which leads to an appreciable decrease in the intensity of transitions corresponding to ionization of the $2b_1$ and $7b_2$ orbitals, followed by the appearance of related satellites. Another example of intense satellite formation is breakdown of the orbital ionization picture for the high-energy π orbital $1b_1$. As a result, the corresponding main line is not observed, while all its intensity is distributed between the satellites in the region of ~15.1–16.2 eV of the experimental spectrum.

The spectral envelope calculated by the IP-ADC(3)/aug-cc-pVTZ method was in good qualitative agreement with the recently obtained photoelectron spectrum of γ-pyrone [8], which made it possible to assign the observed bands. Our results significantly change the interpretation of the spectrum available in the literature and based on SAC-CI calculations [8], which predicts the absence of satellites throughout the entire outer-valence range of ionization of γ-pyrone. Furthermore, this gives reason to believe that the SAC-CI method and equivalent IP-EOM-CCSD approximation have certain problems related to the description of $2h$–$1p$ states, which require special theoretical analysis.

The sequence of six lowest transitions in the ionization spectrum was reliably determined by the CC3 method and energy extrapolation to the complete basis set limit. The obtained results are quantitatively consistent with the experimental data, according to which the vertical gap between the 1^2B_2 ($8b_2^{-1}$) and 1^2B_1 ($3b_1^{-1}$) lowest cationic states of γ-pyrone amounts to 0.25 eV. This suggests the possibility of their vibronic interaction which should be taken into account while studying the vibronic structure of photoelectron transitions.

AUTHOR INFORMATION

A.B. Trofimov, ORCID: https://orcid.org/0000-0003-3523-7086

E.K. Iakimova, ORCID: https://orcid.org/0000-0002-6534-7553

E.V. Gromov, ORCID: https://orcid.org/0000-0003-1176-026X

A.D. Skitnevskaya, ORCID: https://orcid.org/0000-0002-9328-1598

FUNDING

This study was performed under financial support from the Russian Science Foundation (project no. 23-23-00485; https://rscf.ru/project/23-23-00485/).

CONFLICT OF INTEREST

The authors of this work declare that they have no conflicts of interest.

OPEN ACCESS

REFERENCES

1. Wilk, W., Waldmann, H., and Kaiser, M., *Bioorg. Med. Chem*., 2009, vol. 17, p. 2304. https://doi.org/10.1016/j.bmc.2008.11.001
2. Lauridsen, J.M.V., Kragh, R.R., and Lee, J.-W., *Comprehensive Heterocyclic Chemistry IV*, Maulide, N., Ed., New York: Elsevier: 2022, vol. 7, p. 329. https://doi.org/10.1016/B978-0-12-818655-8.00005-6
3. Xu, Y.-L., Teng, Q.-H., Tong, W., Wang, H.-S., Pan, Y.-M., and Ma, X.-L., *Molecules*, 2017, vol. 22, article no. 109. https://doi.org/10.3390/molecules22010109
4. Zantioti-Chatzouda, E.-M., Kotzabasaki, V., and Stratakis, M., *J. Org. Chem*., 2022, vol. 87, p. 8525. https://doi.org/10.1021/ acs.joc.2c00627

5. Peng, X.-P., Li, G., Ji, L.-X., Li, Y.-X., and Lou, H.-X., *Nat. Prod. Res*., 2020, vol. 34, p. 1091. https://doi.org/10.1080/14786419.2018.1548462
6. Gotsko, M.D., Saliy, I.V., Sobenina, L.N., Ushakov, I.A., and Trofimov, B.A., *Tetrahedron Lett*., 2019, vol. 60, article ID 151126. https://doi.org/10.1016/j.tetlet.2019.151126
7. Gotsko, M.D., Saliy, I.V., Sobenina, L.N., Ushakov, I.A., Kireeva, V.V., and Trofimov, B.A., *Synthesis*, 2022, vol. 54, p. 1134. https://doi.org/10.1055/a-1681-4164
8. Palmer, M.H., Coreno, M., De Simone, M., Grazioli, C., Jones, N.C., Hoffmann, S.V., Aitken, R.A., and Sonecha, D.K., *J. Chem. Phys*., 2023, vol. 158, article ID 014304. https://doi.org/10.1063/5.0128764
9. Cederbaum, L.S., Domcke, W., Schirmer, J., and Von Niessen, W., *Adv. Chem. Phys*., 1986, vol. 65, p. 115. https://doi.org/10.1002/9780470142899.ch3
10. Nakatsuji, H. and Hirao, K., *J. Chem. Phys*., 1978, vol. 68, p. 2053. https://doi.org/10.1063/1.436028
11. Nakatsuji, H., *Chem. Phys. Lett*., 1979, vol. 67, p. 334. https://doi.org/10.1016/0009-2614(79)85173-8
12. Ehara, M., Hasegawa, J., and Nakatsuji, H., *Theory and Applications of Computational Chemistry*, Dykstra, C.E., Frenking, G., Kim, K.S., and Scuseria, G.E., Eds., New York: Elsevier, 2005, p. 1099. https://doi.org/10.1016/B978-044451719-7/50082-2
13. Schirmer, J., Cederbaum, L.S., and Walter, O., *Phys. Rev. A*, 1983, vol. 28, p. 1237. https://doi.org/10.1103/PhysRevA.28.1237
14. Schirmer, J., Trofimov, A.B., and Stelter, G., *J. Chem. Phys*., 1998, vol. 109, p. 4734. https://doi.org/10.1063/1.477085
15. Dempwolff, A.L., Paul, A.C., Belogolova, A.M., Trofimov, A.B., and Dreuw, A., *J. Chem. Phys*., 2020, vol. 152, p. article ID 024113. https://doi.org/10.1063/1.5137792
16. Patanen, M., Abid, A.R., Pratt, S.T., Kivimäki, A., Trofimov, A.B., Skitnevskaya, A.D., Grigoricheva, E.K., Gromov, E.V., Powis, I., and Holland, D.M.P., *J. Chem. Phys*., 2021, vol. 155, article ID 0058983. https://doi.org/10.1063/5.0058983
17. Trofimov, A.B., Holland, D.M.P., Powis, I., Menzies, R.C., Potts, A.W., Karlsson, L., Gromov, E.V., Badsyuk, I.L., and Schirmer, J., *J. Chem. Phys*., 2017, vol. 146, article no. 244307. https://doi.org/10.1063/1.4986405
18. Nooijen, M. and Bartlett, R.J., *J. Chem. Phys*., 1995, vol. 102, p. 3629. https://doi.org/10.1063/1.468592
19. Sinha, D., Mukhopadhya, D., Chaudhuri, R., and Mukherjee, D., *Chem. Phys. Lett*., 1989, vol. 154, p. 544. https://doi.org/10.1016/0009-2614(89)87149-0
20. Stanton, J.F. and Gauss, J., *J. Chem. Phys*., 1994, vol. 101, p. 8938. https://doi.org/10.1063/1.468022
21. Trofimov, A.B., Schirmer, J., Holland, D.M.P., Karlsson, L., Maripuu, R., Siegbahn, K., and Potts, A.W., *J. Chem. Phys*., 2001, vol. 263, p. 167. https://doi.org/10.1016/S0301-0104(00)00334-7
22. Krishnan, R., Binkley, J.S., Seeger, R., and Pople, J.A., *J. Chem. Phys*., 1980, vol. 72, p. 650. https://doi.org/10.1063/1.438955
23. Clark, T., Chandrasekhar, J., Spitznagel, G.W., and Schleyer, P.v.R., *J. Comput. Chem*., 1983, vol. 4, p. 294. https://doi.org/10.1002/jcc.540040303
24. Dunning, T.H., *J. Chem. Phys.*, 1989, vol. 90, p. 1007. https://doi.org/10.1063/1.456153
25. Kendall, R.A., Dunning, T.H., and Harrison, R.J., *J. Chem. Phys*., 1992, vol. 96, p. 6796. https://doi.org/10.1063/1.462569
26. Shao, Y., Gan, Z., Epifanovsky, E., Gilbert, A.T.B., Wormit, M., Kussmann, J., Lange, A.W., Behn, A., Deng, J., Feng, X., Ghosh, D., Goldey, M., Horn, P.R., Jacobson, L.D., Kaliman, I., Khaliullin, R.Z., Kuś, T., Landau, A., Liu, J., Proynov, E.I., Rhee, Y.M., Richard, R.M., Rohrdanz, M.A., Steele, R.P., Sundstrom, E.J., Woodcock, H.L., Zimmerman, P.M., Zuev, D., Albrecht, B., Alguire, E., Austin, B., Beran, J.O.G., Bernard, Y.A., Berquist, E., Brandhorst, K., Bravaya, K.B., Brown, S.T., Casanova, D., Chang, C.M., Chen, Y., Chien, S.H., Closser, K.D., Crittenden, D.L., Diedenhofen, M., DiStasio, R.A., Do, H., Dutoi, A.D., Edgar, R.G., Fatehi, S., Fusti-Molnar, L., Ghysels, A., Golubeva-Zadorozhnaya, A., Gomes, J., Hanson-Heine, M.W.D., Harbach, P.H.P., Hauser, A.W., Hohenstein, E.G., Holden, Z.C., Jagau, T.-C., Ji, H., Kaduk, B., Khistyaev, K., Kim, J., Kim, J., King, R.A., Klunzinger, P., Kosenkov, D., Kowalczyk, T., Krauter, C.M., Lao, K.U., Laurent, A.D., Lawler, K.V., Levchenko, S.V., Lin, C.Y., Liu, F., Livshits, E., Lochan, R.C., Luenser, A., Manohar, P., Manzer, S.F., Mao, S.-P., Mardirossian, N., Marenich, A.V., Maurer, S.A., Mayhall, N.J., Neuscamman, E., Oana, C.M., Olivares-Amaya, R., O'Neill, D.P., Parkhill, J.A., Perrine, T.M., Peverati, R., Prociuk, A., Rehn, D.R., Rosta, E., Russ, N.J., Sharada, S.M., Sharma, S., Small, D.W., Sodt, A., Stein, T., Stück, D., Su, Y.-C., Thom, A.J.W., Tsuchimochi, T., Vanovschi, V., Vogt, L., Vydrov, O., Wang, T., Watson, M.A., Wenzel, J., White, A., Williams, C.F., Yang, J., Yeganeh, S., Yost, S.R., You, Z.-Q., Zhang, I.Y., Zhang, X., Zhao, Y., Brooks, B.R., Chan, G.K.L., Chipman, D.M., Cramer, C.J., Goddard, W.A. III, Gordon, M.S., Hehre, W.J., Klamt, A., Schaefer, H.F., Schmidt, M.W., Sherrill, C.D., Truhlar, D.G., Warshel, A., Xu, X., Aspuru-Guzik, A., Baer, R., Bell, A.T., Besley, N.A., Chai, J.-D., Dreuw, A., Dunietz, B.D., Furlani, T.R., Gwaltney, S.R., Hsu, C.P., Jung, Y., Kong, J., Lambrecht, D.S., Liang, W., Ochsenfeld, C., Rassolov, V.A., Slipchenko, L.V.,

Subrelik, J.E., Van Voorhis, T., Herbert, J.M., Krylov, A.I., Gill, P.M.W., and Head-Gordon, M., *Mol. Phys*., 2015, vol. 113, p. 184. https://doi.org/10.1080/00268976.2014.952696

27. Frisch, M.J., Trucks, G.W., Schlegel, H.B., Scuseria, G.E., Robb, M.A., Cheeseman, J.R., Scalmani, G., Barone, V., Petersson, G.A., Nakatsuji, H., Li, X., Caricato, M., Marenich, A.V., Bloino, J., Janesko, B.G., Gomperts, R., Mennucci, B., Hratchian, H.P., Ortiz, J.V., Izmaylov, A.F., Sonnenberg, J.L., Williams-Young, D., Ding, F., Lipparini, F., Egidi, F., Goings, J., Peng, B., Petrone, A., Henderson, T., Ranasinghe, D., Zakrzewski, V.G., Gao, J., Rega, N., Zheng, G., Liang, W., Hada, M., Ehara, M., Toyota, K., Fukuda, R., Hasegawa, J., Ishida, M., Nakajima, T., Honda, Y., Kitao, O., Nakai, H., Vreven, T., Throssell, K., Montgomery, J.A., Jr., Peralta, J.E., Ogliaro, F., Bearpark, M., Heyd, J.J., Brothers, E., Kudin, K.N., Staroverov, V.N., Keith, T.A., Kobayashi, R., Normand, J., Raghavachari, K., Rendell, A., Burant, J.C., Iyengar, S.S., Tomasi, J., Cossi, M., Millam, J.M., Klene, M., Adamo, C., Cammi, R., Ochterski, J.W., Martin, R.L., Morokuma, K., Farkas, O., Foresman, J.B., and Fox, D.J., *Gaussian 16. Revision A.03*, Wallingford CT: Gaussian, 2016
28. Schaftenaar, G., Vlieg, E., and Vriend, G., *J. Comput.-Aided Mol. Des*., 2017, vol. 31, p. 789. https://doi.org/10.1007/s10822-017-0042-5
29. Christiansen, O., Koch, H., and Jørgensen, P., *J. Chem. Phys*., 1995, vol. 103, p. 7429. https://doi.org/10.1063/1.470315
30. Koch, H., Jensen, H.J.A., Jørgensen, P., and Helgaker, T., *J. Chem. Phys*., 1990, vol. 93, p. 3345. https://doi.org/10.1063/1.458815
31. Koch, H. and Jørgensen, P., *J. Chem. Phys*., 1990, vol. 93, p. 3333. https://doi.org/10.1063/1.458814
32. Stanton, J.F., Gauss, J., Cheng, L., Harding, M.E., Matthews, D.A., Szalay, P.G., et al., CFOUR, Coupled Cluster Techniques for Computational Chemistry, a Quantum Chemical Program Package. https://cfour.uni-mainz.de/cfour/
33. Von Niessen, W., Schirmer, J., and Cederbaum, L.S., *Comput. Phys. Rep*., 1984, vol. 1, p. 57. https://doi.org/10.1016/0167-7977(84)90002-9
34. Zakrzewski, V.G. and Ortiz, V., *Int. J. Quantum Chem*., 1994, vol. 52, p. 23. https://doi.org/10.1002/qua.560520806
35. Zakrzewski, V.G. and Von Niessen, W., *J. Comput. Chem*., 1993, vol. 14, p. 13. https://doi.org/10.1002/jcc.540140105
36. Feller, D., *J. Chem. Phys*., 1992, vol. 96, p. 6104. https://doi.org/10.1063/1.462652
37. Feller, D., *J. Chem. Phys*., 1993, vol. 98, p. 7059. https://doi.org/10.1063/1.464749